DOI: 10.13140/RG.2.2.30320.38403

Reconstructing a Soviet-Era Plastic Model to Predict Vibratory Pile Driving Performance

Don C. Warrington, PhD, P.E.
University of Tennessee at Chattanooga
Department of Mechanical Engineering

The technique for driving piles by vibration (as opposed to impact) has been an important component of deep foundations and retaining wall installation since it was first demonstrated in the Soviet Union in the late 1940's. The Soviets originally developed the technology and applied it to a wide variety of pile types. Nevertheless, the analytical methods they developed to estimate the performance of these machines have not been widely disseminated outside of the country, either before or after the breakup of the Soviet Union. In this paper one specific model, analysing longitudinal vibratory performance using a purely plastic/Coulombic model of soil resistance, is reconstructed and discussed. The model is compared with the most disseminated Soviet model for sizing vibratory pile drivers and predicting performance. Some discussion on Soviet vibratory modelling beyond the model presented is also included.

Keywords: vibratory pile driving, Soviet Union, Savinov and Luskin method, numerical modelling

Introduction

The beginnings and development of vibratory technology for the installation of piles is a story that has been documented elsewhere (Tseitlin, Verstov, and Azbel (1987); Warrington (1992).) The productivity improvements in its use, especially with the installation of sheet piling and large diameter casings, represent a significant advance in construction technology.

As is the case with impact driven piles, it is desirable to predict the performance of vibratory pile drivers in use and, for piles that must bear axial or lateral loads, their deflection response to those loads. The challenges with vibratory technology towards that end are daunting in that the vibration of the pile induces significant changes in the surrounding soil during and after installation, which significantly complicate estimating either driving performance or the load-settlement characteristics of the pile during use. Research to quantify these phenomena has gone on for many years (A. Holeyman, Bertin, and Whenham (2013); A. E. Holeyman (2000); Massarsch, Fellenius, and Bodare (2017); Viking (2002).) At this point, however, a consensus does not exist concerning the axial capacity of piles driven by vibration.

With continued interest in this and related topics such as vibratory compaction (deep and shallow) it is interesting to consider models that came from the original effort to develop the technology, namely that in the Soviet Union, where a great deal of research an equipment development took place in the years bracketing what they refer to as the "Great Patriotic War." Some of the early history of Soviet development of vibratory pile driving equipment–and the parallel impact-vibration equipment–was documented by Barkan (1957). His own research started in 1934; like the wave equation analysis for impact piles, getting its initial analysis in Australia and the UK during the same period, it was interrupted by same Great Patriotic War. After that was concluded, the development continued: in 1949, the Soviet BT-5 vibrator was used to install flat sheeting for a cellular cofferdam during the construction of the Gorky (now again Nizhni-Novgorod) hydroelectric facility. A view of the internal construction of this vibrator is shown in Figure 1. The vibrator installed these piles 9-12 m into saturated sand in 2-3 minutes.

Barkan (1957) furnishes additional information on early Soviet vibrators and the projects they were used on. Other information along these lines is given by Levkin (1960).

In spite of these sources, much of the literature published inside of the Soviet Union has not been well disseminated outside of the country, although Gumenskii and Komarov (1959) is an exception. Over the years we have attempted to disseminate as much of this information as possible, including translation of portions of Tseitlin et al. (1987).

It is one of those portions–the original, "simple" model of longitudinal vibration into a purely plastic soil both along the shaft and at the toe–that is the subject of this paper. In this we will attempt to reconstruct the model, automate its execution and extend it a bit to related topics. In the process it is hoped that the detailed discussion of this model will increase understanding of the mechanism of vibratory pile driving, and give a greater appreciation for those who first developed the technology.

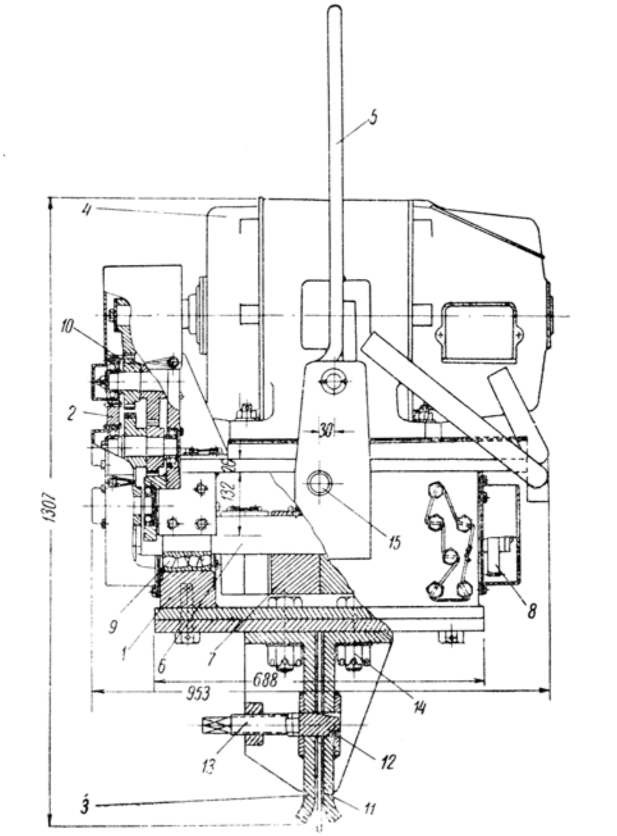

Figure 1. BT-5 Vibrator (from Savinov and Luskin (1960))

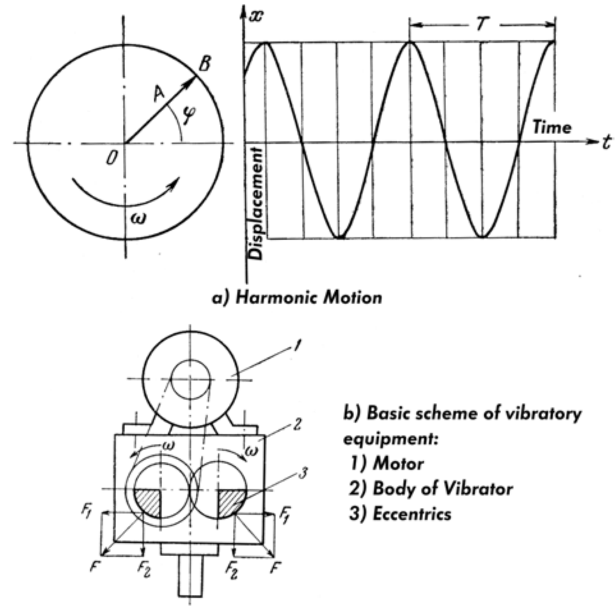

Figure 2. Basics of Vibratory Technology and Pile Drivers (modified from Rebrik (1966))

Before we get into the topic itself: since this is a model reconstruction rather than original research (although some of that will appear as well,) a more informal, educational tone will be used. We trust that this does not present a problem.

Vibratory Pile Driving and Model Basics

Vibratory pile driving–and all other vibratory technology–is based on the application of a harmonic force to a system to induce some kind of harmonic displacement. This is illustrated in Figure 2(a).

A vibratory pile driver is shown schematically in Figure 2(b). The harmonic force is produced by rotating the eccentrics at an angular velocity ω; the eccentrics rotate in such a way that the horizontal forces cancel each other out and the vertical ones produce a force whose peak value is

$$P_o = K\omega^2 \quad (1)$$

For the "free hanging" case where there is no other resistance to the force other than the vibrating mass of the system, the equation of motion is

$$m_o \frac{d^2}{dt^2} x(t) = -P_o \sin(\phi) \quad (2)$$

where

$$\phi = \omega t + \alpha \quad (3)$$

Although this equation isn't very useful *per se*, its solution is used to define many vibratory parameters on a practical basis. These are discussed at length in Warrington (1992).

Turning to our current task, Tseitlin et al. (1987) begin their presentation with the addition of soil resistance to this model, as shown in Figure 3.

This expands Equation 2 to

$$m_o \frac{d^2}{dt^2} x(t) = -P_o \sin(\omega t + \alpha) + i_1 Q + i_2 F + i_3 R \quad (4)$$

The indices i_1, i_2, i_3 can be valued -1, 0 or 1 depending upon the direction of the velocity at different stages of the cycle. The force Q is the gravity force on the system and thus $i_1 = 1$ always. The other two are in opposite direction to the system velocity.

At this point Tseitlin et al. (1987) made five key assumptions that need to be understood:

1. The pile and vibrator clamped together are a rigid body. This assumption has held up well for a great deal of subsequent vibratory analysis, as the $^L/_c$ of the pile is generally much smaller than the exciting period T.

2. The soil surrounding the pile is immobile, which will be discussed shortly.

3. The soil force F acting on both the pile shaft is a dry, purely plastic frictional (Coulombic) force. Tseitlin et al.

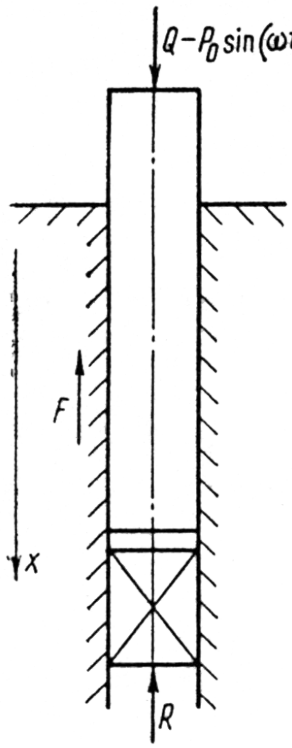

Figure 3. Computational diagram for vibrational driving using longitudinal vibrations (from Tseitlin et al. (1987))

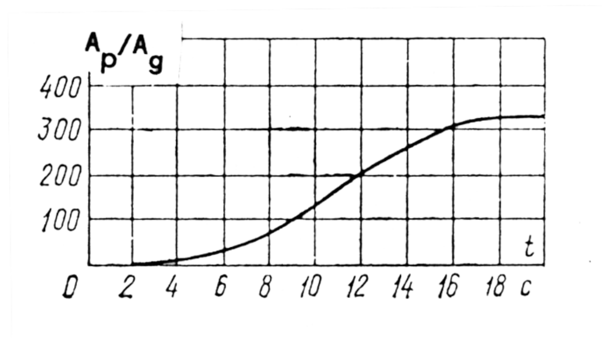

Figure 4. Amplitude Ratio vs. Time Between Pile and Ground (from Tseitlin et al. (1987))

(1987) claim that this assumption had experimental verification, and that the elastic component was negligible at high speed penetration of the pile.

4. The toe resistance R was constant at all times when the toe of the pile penetrated the soil under it. This is probably the weakest assumption made; however, the model shows very clearly that, for much of the vibratory cycle, the pile is lifted from and not engaging the toe, a point made by Massarsch et al. (2017), who discuss the way this intermittent engagement affects the toe resistance of the pile depending upon the way driving is stopped.

5. The vibrator acts on the pile with a sinusoidal force in accordance with the right hand side of Equation 2. One interesting point they discuss–and it is seldom mentioned in the literature–is the additional assumption that ω is constant. They make the point that both their theoretical and experimental research showed that ω varied by about 5%. For this reason they continued their assumption of a constant ω. Further discussion of this issue can be found in Warrington (2006).

Tseitlin et al. (1987) also presented Figure 4, which they explained as follows:

> Experimental research has established that the amplitude of the vibrations A_g of the ground surrounding the pile is comparable to the amplitude of the pile being sunk only during the initial stage in which the pile vibrates together with the ground. As breakthrough progresses, the ground vibrations diminish, while those of the pile increase; in the final stage of breakthrough, the ratio of the amplitude of the pile's vibrations to that of the ground vibrations reaches two to three orders of magnitude, which also permits us to consider the ground surrounding the pile immobile during the sinking process.
>
> To illustrate the above, a graph of the characteristic is presented in (Figure 4,) which shows the progress of breakthrough over time during the sinking of a steel pipe whose vibration amplitude A_p is more than 300 times greater than A_g by at the end of breakthrough and toward the beginning of the actual sinking process.

Anyone who has witnessed vibratory pile understands the "breakthrough" they were talking about and the increase in penetration speed that results from that after the driver is started. What can also be observed, albeit in an informal, qualitative way, is that this diagram looks suspiciously like the mirror image of Figure 5, which shows the effect of strain softening on the shear modulus of soils. The application of strain softening theory to vibratory pile driving is a significant advance in our understand of this phenomena. Strain softening in a different context is discussed in Warrington (2019a, 2019b).

Solution of the Equations of Motion

Although Tseitlin et al. (1987) state the equations of motion in detail, they do not solve them. In order to attempt replication their results, it will be necessary to solve these equations, starting with the basic equation of motion, Equation 4. In order to generalise the results, it will be necessary to convert Equation 4 to a dimensionless form. This is done in three stages.

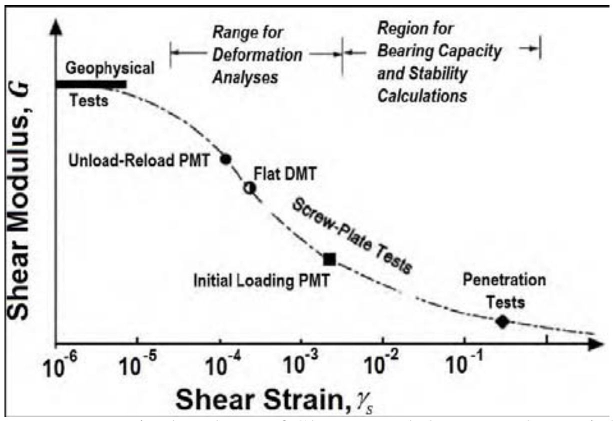

Figure 5. Typical Values of Shear Modulus Based on Field Tests (from Loehr, Lutenegger, Rosenblad, and Boeckmann (2016))

The first stage is to employ the same technique as used in Warrington (2020): transform the time variable using the characteristic frequency of the system. This is done as follows:

$$\tau = \omega t \tag{5}$$

$$\begin{aligned} X(\tau) &= x(\omega t) \\ \frac{d}{d\tau} X(\tau)\omega &= \frac{d}{dt} x(\omega t) \\ \frac{d^2}{d\tau^2} X(\tau)\omega^2 &= \frac{d^2}{dt^2} x(\omega t) \end{aligned} \tag{6}$$

Such transformations are discussed in Bronshtein and Semendyayev (1971). It is interesting to note that, even though Warrington (2020) is a free vibration problem and this is a forced one, the solution technique contains the same key transformation in both cases.

The second stage is to make the force parameters dimensionless, and this is done as follows:

$$\begin{aligned} q &= \frac{Q}{P_o} \\ f &= \frac{F}{P_o} \\ \gamma &= \frac{R}{P_o} \end{aligned} \tag{7}$$

Applying Equations 5, 6 and 7 to Equation 4 yields

$$\frac{m_o\,\omega^2 \frac{d^2}{d\tau^2} X(\tau)}{P_o} = -\sin(\tau + \alpha) + i_1 q + i_2 f + i_3 \gamma \tag{8}$$

The final stage is to apply the following transformation to the left hand side:

$$y(\tau) = \frac{m_o\,\omega^2 X(\tau)}{P_o} \tag{9}$$

Doing this, we have at last

$$\frac{d^2}{d\tau^2} y(\tau) = -\sin(\tau + \alpha) + i_1 q + i_2 f + i_3 \gamma \tag{10}$$

This equation applies to the entire cycle; however, due to the changes in the direction of the forces, the solution for the entire cycle is to be piecewise.

As was the case with Warrington (2020), Laplace transforms can be employed for this solution. The Laplace transform for Equation 10 is

$$s\,(s\mathcal{L}(y(\tau), \tau, s) - y(0)) - \mathrm{D}(y)(0) = -\frac{s\sin(\alpha) + \cos(\alpha)}{s^2 + 1} + \frac{i_1 q}{s} + \frac{i_2 f}{s} + \frac{i_3 \gamma}{s} \tag{11}$$

Solving for the transformed variable and taking the inverse transform yields

$$\begin{aligned} y(\tau) = {} & 1/2\left(i_1 q \tau^2 + i_3 \gamma \tau^2 + i_2 f \tau^2\right) + \\ & \mathrm{D}(y)(0)\tau - \cos(\alpha)\tau + \sin(\alpha)\cos(\tau) + \\ & \cos(\alpha)\sin(\tau) + y(0) - \sin(\alpha) \end{aligned} \tag{12}$$

At this point we must face an important fact: since this is a piecewise solution, the initial conditions are not going to be the same for each 'piece.' If we assume for each piece the initial time to be τ_o, the initial velocity to be v_o and the initial displacement to be y_o, and employing the phase shifting technique as described in Kreyszig (1988), the complete solution is

$$\begin{aligned} y(\tau) = {} & 1/2\left(i_1 q \tau^2 + i_3 \gamma \tau^2 + i_2 f \tau^2\right) + \tau v_o - \tau i_1 q \tau_0 - \tau i_3 \gamma \tau_0 - \tau i_2 f \tau_o + \\ & \tau \sin(\alpha)\sin(\tau_0) - \tau \cos(\alpha)\cos(\tau_0) + \sin(\alpha)\cos(\tau) + \cos(\alpha)\sin(\tau) + \\ & y_o + 1/2\, i_1 q {\tau_0}^2 + 1/2\, i_3 \gamma {\tau_0}^2 + 1/2\, i_2 f \tau_0^2 - \tau_0 v_o - \\ & \tau_0 \sin(\alpha)\sin(\tau_0) + \tau_0 \cos(\alpha)\cos(\tau_0) - \sin(\alpha)\cos(\tau_0) - \cos(\alpha)\sin(\tau_0) \end{aligned} \tag{13}$$

The dimensionless velocity is

$$\begin{aligned} \frac{d}{d\tau} y(\tau) = {} & i_1 q \tau + i_3 \gamma \tau + i_2 f \tau + v_o - i_1 q \tau_0 - i_3 \gamma \tau_0 - i_2 f \tau_0 + \\ & \sin(\alpha)\sin(\tau_0) - \cos(\alpha)\cos(\tau_0) - \sin(\alpha)\sin(\tau) + \cos(\alpha)\cos(\tau) \end{aligned} \tag{14}$$

and the dimensionless acceleration is

$$\frac{d^2}{d\tau^2} y(\tau) = i_1 q + i_3 \gamma + i_2 f - \sin(\alpha)\cos(\tau) - \cos(\alpha)\sin(\tau) \tag{15}$$

Implementing the Solution

The equations of motion solved, we now can proceed to implement the solution. Up until now we have implicitly favoured a true piecewise solution; however, a numerical solution using Equation 4 would be more natural. There are three reasons why we continue to opt for a piecewise solution, or solution by stages:

1. Since this is supposed to be a reconstruction of the original, a piecewise solution would be more realistic in that role. In any case, producing Equations 13, 14 and 15 give a greater appreciation for the original effort, which was doubtless done by hand.

2. Purely plastic models pose stability problems for discrete numerical solutions because they create an absolute discontinuity at the point of zero velocity. This is analogous to shock waves in computational fluid dynamics, which have bedevilled solutions of those problems for many years. Although elasto-plastic models have their own problems with non-smooth transition points, they are more easily manageable than those of purely plastic, Coulombic solutions.

3. They give additional insight into the different stage of motion that the hammer-pile-soil system undergoes during the vibratory cycle.

There are five basic stages of motion the system undergoes during the cycle:

1. Raising stage, where the system starts from rest at $\tau_1 = 0$, $\phi_1 = \alpha$, $y_1 = 0$, $v_1 = 0$. This ends at τ_2 when the upward momentum of the system is unable to overcome the opposing forces of gravity and shaft friction, and the system comes to a halt.

2. Upper parking stage, where the system continues at rest until the force of the eccentric is able to move the system downward against the shaft friction and with gravity, or the right hand side of Equation 8 is less than zero. Here $\phi_2 = \tau_2 + \alpha$, $v_2 = 0$.

3. First downward stage, starting at the point where the right hand side of Equation 8 is equal to zero, after which the system travels downward until it first impacts the soil plug at the pile toe. Here $\phi_3 = \tau_3 + \alpha$, $v_3 = 0$, $y_3 = y_2$.

4. Second downward stage, where the system penetrates the soil plug at the pile toe until that resistance, in combination with the shaft resistance, brings the system to a halt. Here $\phi_4 = \tau_4 + \alpha$, $y_4 = 0$.

5. Lower parking stage, where the system stops until (or at) $\phi = \alpha$. The system remains parked until the right hand side of Equation 8 equals zero. Here $\phi_5 = \tau_5 + \alpha$, $y_5 = y_{max}$, $v_5 = 0$. At the end of this stage the displacement is reset and the cycle begins again.

It should be noted that, depending upon the values of q, f and γ, either or both parking stages can be eliminated from a particular case. The parking stages are the result of the purely plastic model, and reduce the problem of numerical instability from the solution.

Since Equations 13, 14 and 15 do not use the velocity to determine the direction or even the relevance of q, f or γ to a specific stage, it is necessary to use the index i_n. Values for these are shown in Table 1.

Up to now we have not discussed the phase angle α. This is because it is determined at the end of the cycle; in effect we start at the end and work backwards. If we apply the condition for the lower parking stage (Stage 5,) the appropriate values for i_n, and the fact that at the end of the cycle $\tau_1 = 0$ to Equation 8, we have

Table 1
Direction Indices for Various Stages of Motion

Stage	i_1	i_2	i_3
1	+1	+1	0
2	+1	-1	0
3	+1	-1	0
4	+1	-1	-1
5	+1	+1	0

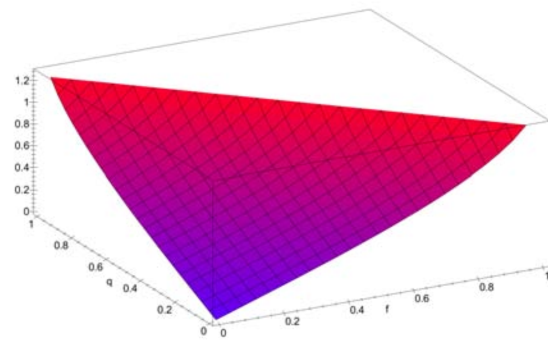

Figure 6. Phase Angle α, Radians

$$\sin(\alpha) = q + f \tag{16}$$

from which

$$\alpha = \arcsin(q + f) \tag{17}$$

This is graphically represented in Figure 6. The diagonal division is a result of the physics of the system. At the starting point τ_1, if in fact the sum of the gravity force and the resisting shaft friction are greater than the dynamic force of the eccentrics ($q + f \geq 1$,) the system will not raise at all.

To solve for each of these stages, it is necessary to determine the initial times τ_n, from which Equations 13 and 14 could be solved using this and the initial conditions of each stage. In most cases it was necessary to use Newton's Method to determine τ_n. In some cases the equations had no explicit solution; in others, using an explicit solution returned a principal value for an angle, which was frequently not applicable to the stage at hand. Obtaining the times τ_n was one of the most difficult aspects of this model, and was not always successful, especially with marginal cases.

Computing the Power Consumption

One place where we will expand the information obtained from the model is an estimate of the power consumption. This topic is discussed in depth in Warrington (1994, 2006).

From these sources, to summarise in brief, the power consumption can be estimated by the following formula:

$$N = \alpha_p \frac{K^2 \omega^3}{m_o} = \alpha_p \frac{P_o^2}{\omega m_o} \tag{18}$$

The determination of α_p is complicated by three factors.

The first is the inclusion or exclusion of other losses in the system; Equation 18, for example, does not automatically include any consideration of internal losses in the vibrating machinery. This is of special interest to equipment designers and manufacturers but also to those who would use the power usage of the system to monitor its performance.

The second is the way in which the system uses that power, which in turn relates to the interaction of the torque delivered to the system with its requirements. This has already been mentioned relative to the rotational speed stability of the system.

The third–and probably the most important–is the fact that the values of α_p computed for Equation 18 in Warrington (1994, 2006) assume a simple dashpot to model the soil resistance. Although this is not particularly useful to estimate the driving performance of the system, it is a reasonable first estimate, and has the additional advantage that there is a theoretical maximum for the power, namely $\alpha_p = 0.25$, from which Equation 18 becomes

$$N = \frac{K^2 \omega^3}{4 m_o} = \frac{P_o^2}{4 \omega m_o} \tag{19}$$

Although this result is derived in Warrington (1994, 2006), Savinov and Luskin (1960) note that this result was originally obtained in the 1950's.

For equipment manufacturers this is a useful baseline from which adjustments can be made. However, while viscous and Coulombic damping can be related (James, Smith, Wolford, and Whaley (1989)) the relationship is not perfect and in any case does not consider the effects of the pile toe.

However, the underlying theory can be used to adapt this model for estimation of power consumption. We should start by noting, from Warrington (2006), that the cyclic energy consumed for one cycle (modified for current notation and angle convention) is

$$\Delta E_{cyc} = \int_0^{\frac{2\pi}{\omega}} P_0 \sin(\omega t + \alpha) \frac{d}{dt} x(t)\, dt \tag{20}$$

If we apply the same three transformations that we did to obtain Equation 10, the result is

$$\frac{\Delta E_{cyc} m_o \omega^2}{P_o^2} = \int_0^{2\pi} \sin(\tau + \alpha) \frac{d}{d\tau} y(\tau)\, d\tau \tag{21}$$

If we define

$$\Delta E'_{cyc} = \frac{\Delta E_{cyc} m_o \omega^2}{P_o^2} \tag{22}$$

then

$$\Delta E'_{cyc} = \int_0^{2\pi} \sin(\tau + \alpha) \frac{d}{d\tau} y(\tau)\, d\tau \tag{23}$$

One thing that needs to be noted about Equation 23 is that, as noted earlier, the entire cycle is in stages, and thus the integration needs to be broken up. For each stage of motion, the dimensionless energy consumed is

$$\Delta E'_{cyc_n} = \int_{\tau_n}^{\tau_{n+1}} \sin(\tau + \alpha) \frac{d}{d\tau} y(\tau)\, d\tau \tag{24}$$

and then these must be summed for the entire cycle. For parking stages, since by definition $\frac{d}{d\tau} y(\tau) = 0$, no energy is consumed during these stages. Since for the motion stages $\frac{d}{d\tau} y(\tau)$ is determined by Equation 14, it should be evident that the integration is long and tedious, and will not be spelled out here. It was, however, done and included in the program that was developed to replicate the model.

The cycle energy and power of the system are related by the equation

$$N = \frac{\Delta E_{cyc} \omega}{2\pi} \tag{25}$$

Combining Equations 18, 22 and 25 and solving for α_p yields

$$\alpha_p = \frac{|\Delta E'_{cyc}|}{2\pi} \tag{26}$$

Adding the absolute value to the numerator is necessary because the net result of Equation 24 is negative, as the energy transfer is dissipative to the system.

Comparison with Original Results

The code to replicate the original model was written in FORTRAN 77 with assistance from Maple V Release 4. Tseitlin et al. (1987) used two parametric cases to demonstrate the results of the model, and these will be reproduced using the current code.

Case for Specific Frictional Ratio

The first case is a case for a specific value of f, and the original graph is shown in Figure 7. The current code's representation of the same parametric study is shown in Figure 8. The two results are the same within the accuracy of the graphs. In both cases, as one would expect the displacement of the vibrating system per eccentric cycle decreases with increasing toe resistance. Also, in both cases there is a peak

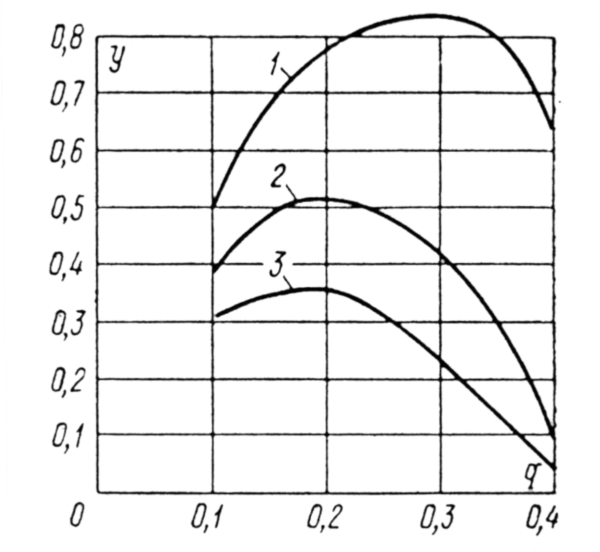

Figure 7. Dimensionless displacement y as a function of parameter q with $f = 0.5$ and 1: $\gamma = 0.7$; 2: $\gamma = 1.0$; 3: $\gamma = 1.3$ (from Tseitlin et al. (1987))

value of displacement for a given range of q. This indicates that there is an optimum value of downward gravity force on the system to enhance driving. For a vibrator with no static (suspension) weight above it, $Q = Q_o$, where

$$Q_o = gm_o \tag{27}$$

and

$$q_o = \frac{Q_o}{P_o} \tag{28}$$

With a static weight on top of the system, $Q > Q_o$, and in fact Tseitlin et al. (1987) state that this result was used to configure statically weighted suspensions for vibratory hammers.

We also applied the model to analyse the coefficient α_p, and this is shown in Figure 9. The values shown are within the $\alpha_p = 0.25$ criterion described earlier. It is also worth noting that, as q increases, the power requirements decrease, which is further justification for the use of a static suspension or down-crowding.

If we divide y by α_p, we obtain the result of Figure 10. For lower values of R, the displacement-power ratio (and by extension the velocity) increases nearly linearly with increasing q. When the toe resistance ratio γ is increased, there is a point at which a peak y/α_p is reached, after which the displacement-power ratio decreases.

As an aside, a specific case contained within these parametric studies can be used to illustrate the detailed output of the code. The tabular data input and results are shown in

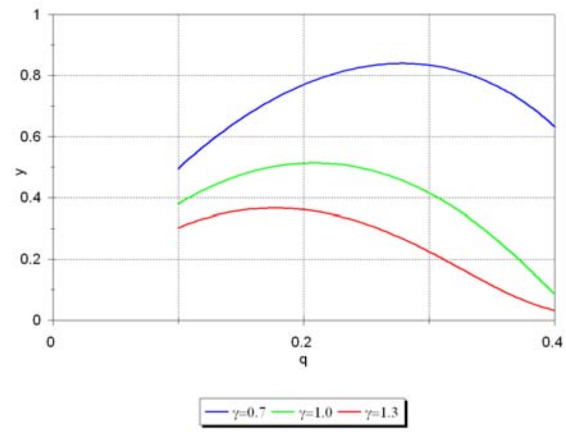

Figure 8. Dimensionless displacement y as a function of parameter q with $f = 0.5$ for different values of γ using current model

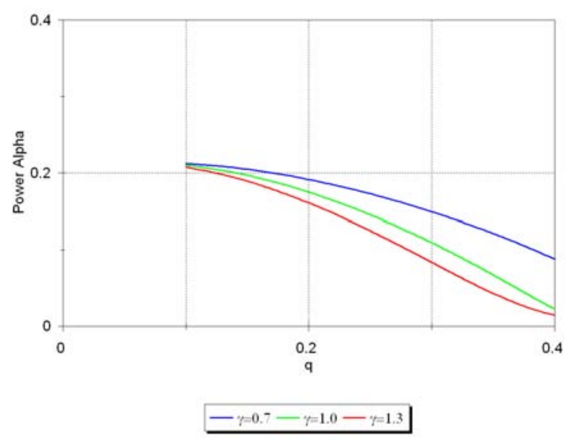

Figure 9. Values of α_p for Parametric Study when $f = 0.5$

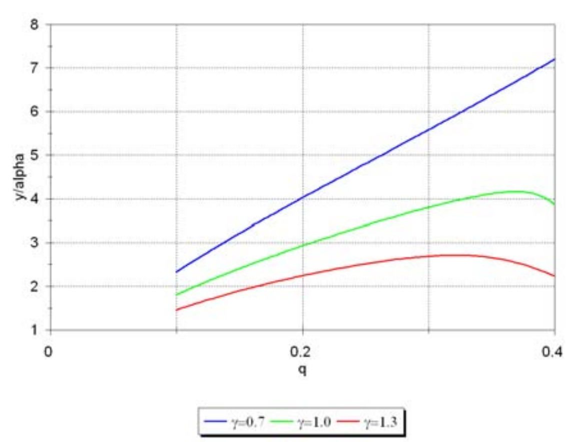

Figure 10. Values of y/α_p for Parametric Study when $f = 0.5$

Table 2
Summary of the Results of Case Study

Parameter	Value
q	0.2
f	0.5
γ	1.0
α, degrees	44.42700
y	0.5133014
ϕ_5, degrees	305.2501
Upper Parking Angle, degrees	12.97632
Lower Parking Angle, degrees	54.74992
α_p	0.1750364
y/α_p	2.932541

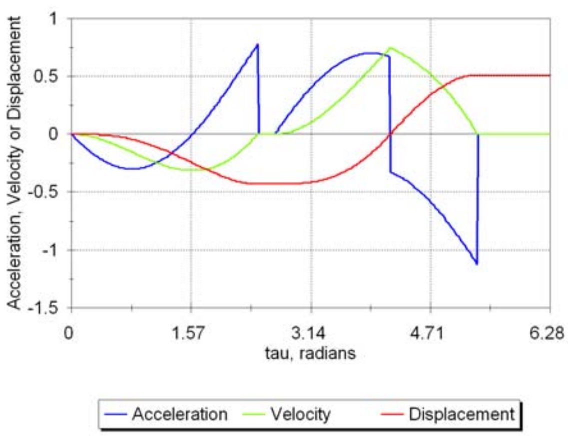

Figure 11. Dimensionless Time History of Case Study

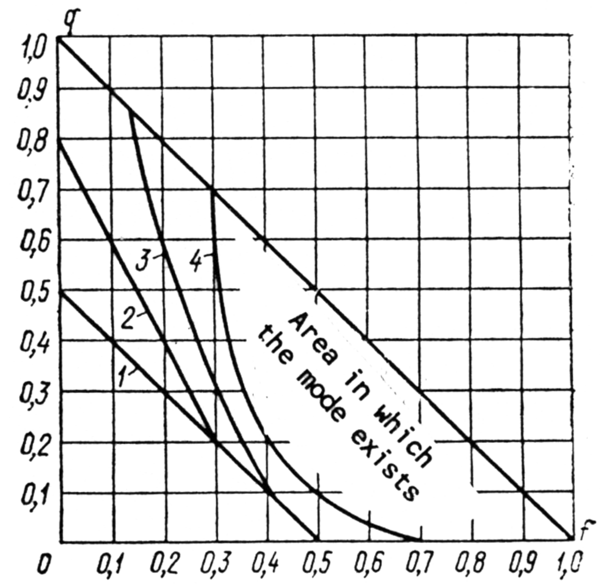

Figure 12. Area in which the mode of pile displacement being studied exists 1: γ = 1.6; 2: γ = 1.3; 3: γ = 1.0; 4: γ = 0.7 (modified from Tseitlin et al. (1987))

Table 2, and a dimensionless time plot of the displacement, velocity and acceleration are shown in Figure 11. It is easy to see with the figure the two parking angle/time regions and the abrupt changes in the velocity and acceleration which in the end lead to a reasonably smooth displacement variation during the cycle.

Parametric Study of Toe Resistance

The second analysis of the method was a parametric study of the performance of the system relative to toe resistance. The original figure is shown in Figure 12. The diagonal across the graph is due to the nature of the phase angle α, which is illustrated in Figure 6. For its part Figure 12 poses two serious problems which need to be resolved in order to understand what is being presented.

The first is the matter of the isoclines themselves: they are drawn in such a way that, in some cases, two different values of γ are represented in one spot. How can this be? Or is it that, at the isocline for γ = 1.6, the whole thing breaks down for all higher values of γ?

The second is more serious yet: what is meant by the expression 'area in which the mode exists?' The Soviets were very conscious that, during vibratory driving, the way the vibrating system interacted with the soil ('the mode') varied with the conditions of driving, especially with changes in the toe resistance relative to shaft resistance. But what specifically are they talking about here?

The results of the code will be presented in a series of 3D contour graphs viewed from the upper right hand corner of Figure 12 and looking towards the origin. There are two types of cases implicit in Figure 12 which are excluded from this analysis. The first are cases along the diagonal (q = f,) which are physically impossible for reasons described earlier. The second are cases where q = 0. In addition to the obvious observation that no vibratory system is without the effect of gravity, vibratory driving systems require the force of gravity to induce net downward motion to the system.

The first graph is the direct analysis of the parameters of Figure 12, which is shown in Figure 13. During the construction of the code model and replication of this parametric study, it became apparent that the isoclines in Figure 12 were in fact minimum values of γ for specific values of f and q below which the model was no longer applicable. For these values of γ, the lower parking angle became zero; lower values of γ made it impossible to 'close the loop' and fulfil the initial and final value match of v required for steady state operation. The most likely source of this situation was the purely plastic model for the toe, which is less realistic than that of the shaft.

Having cleared up that ambiguity, it is necessary to com-

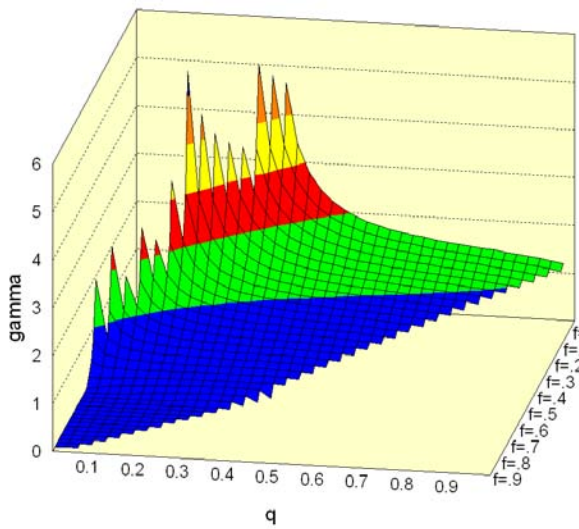

Figure 13. Minimum values of γ with varying values of f and q

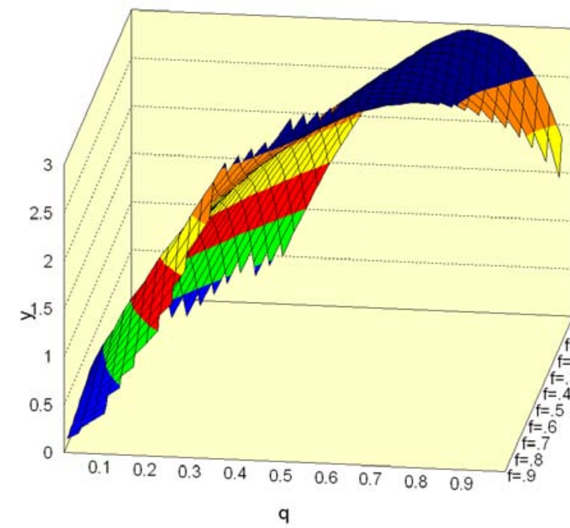

Figure 14. Maximum Displacement for Minimum Values of γ

pare Figures 12 and 13. The simplest way to do that is to observe that, while the two analysis agree qualitatively, quantitatively the two are not quite the same. Both implementation of the model show the same basic region in which 'the mode exists,' up to the point that $\gamma_{min} = 0$ in a region where values of f are very high and values of q very low. The very jagged boundary on the back side of the contour surface reflects the instability of the model as combinations of f and q approach the origin; this was more cleanly (if not more accurately) dealt with in Figure 12's isocline 1. The jagged line at the front shows the instability of the model as the condition $q+f = 1$ is approached. For the code model, it was necessary to review the results and eliminate outliers in the data. The difficulties of the model in extreme conditions are a reminder that, while a time-stepping numerical model was rejected in part to eliminate the problems created by the purely plastic soil model, those problems are also present in this segmented model as well.

Figure 14 shows the values of maximum displacement for these minimum values of γ. It shows that the largest displacements per cycle take place when q is high and f is low, which is unsurprising. It also shows that there is a limit beyond which addition of downward weight is counterproductive, which is the same result shown in Figure 8.

The values of α_p for this parametric study is shown in Figure 15. The graph shows that values for this parameter that exceed the viscous maximum of 0.25 are encountered in a wide range of cases, although for these cases, as was the case in Figure 14, the largest values exist in low values of f (but elevated values of γ.)

The last analysis is the ratio of y to α_p, shown in Figure 16. As was the case above, it shows that the most efficient use of

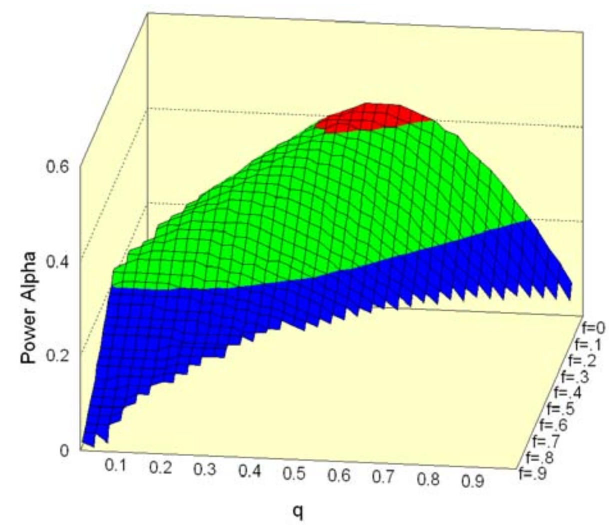

Figure 15. Values of α_p for Minimum Values of γ

the power is in cases where q is high, thus underscoring the addition of static weight to the system.

Relationship with Actual Vibratory Configuration Method

Up to now we have considered the purely plastic model by itself. It would be interesting to see how this can be related to a methodology which attempts to configure (or match) a given vibrator to a given pile-soil system. The method to be studied is the one generally attributed to Savinov and Luskin (1960), but it appears in a number of other publications, such as Erofeev, Smorodinov, Fedorov, Vyazovkii, and Villumsen (1985); Tseitlin et al. (1987); Warrington (1992). This is not intended as yet another outline of the method, but an inter-

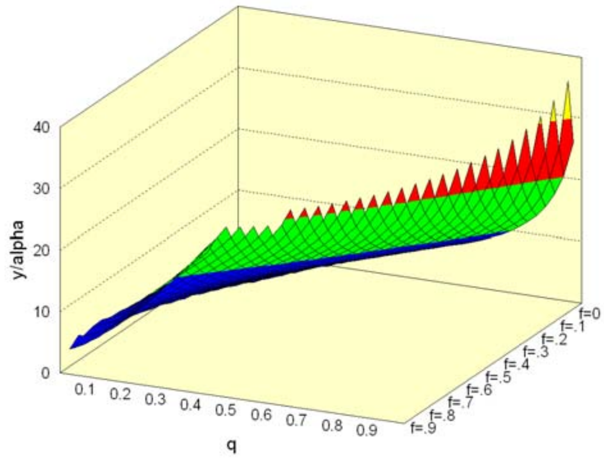

Figure 16. Values of y/α_p for Minimum Values of γ

pretation and summary of the method in light of the cycle analysis method already described.

The basic objectives of this method are to insure that:

1. The dynamic force of the vibrator is sufficient to overcome soil resistance when the pile reaches desired tip elevation;

2. The amplitude of the vibrations are above the minimum amplitude required; and

3. The forces on the pile are sufficient to provide the necessary average sinking speed of the pile.

Starting with the first, the method give typical values of either a) unit soil resistance or b) resistance per unit length of sheet pile to estimate the shaft resistance F'. It then requires that the dynamic force of the vibrator be greater than or equal to the estimated resistance of the pile, or

$$P_o \geq \aleph F' \tag{29}$$

If we define

$$f' = \frac{F'}{P_o} \tag{30}$$

then

$$f' \leq \frac{1}{\aleph} \tag{31}$$

This means that the force ratio may in fact be greater than unity, depending upon the value of $\aleph$. This may seem odd in view of the fact that, as shown earlier, should the equality be achieved the pile will not move upward at the beginning of the eccentric cycle. The use of the primed variable, however, is not accidental; the resistances are likely nominal resistances that could be expected under static loading, and that $f' > f$. Thus it is probable that a reduction in soil resistance during driving would reduce f to levels discussed earlier.

The second objective is achieved in two different ways. The first is to, for a variety of pile and soil combinations, to specify a minimum amplitude A_o and from there estimate the necessary eccentric moment needed. This is done using the formula

$$K \geq \frac{A_o m_o}{\psi} \tag{32}$$

Once this is known, the frequency of the vibrations is determined as

$$\omega = \sqrt{\frac{P_o}{\aleph K}} \tag{33}$$

However, in cases where the pile-soil configuration does not fit into the cases shown, another method of determining the eccentric moment is by invoking an important criterion in this method: the peak, free-hanging velocity should be in the range $0.5\, {}^{m}/_{sec} \leq v_{dyn} \leq 0.8\, {}^{m}/_{sec}$ in order to mobilise the soil and induce the resistance reduction necessary for vibratory driving. To implement this, we note that, from Warrington (1992),

$$v_{dyn} = \frac{gn}{\omega} \tag{34}$$

Noting that

$$n = \frac{P_o}{Q_o} = \frac{P_o}{g m_o} \tag{35}$$

we combine Equations 34 and 35 to yield

$$\omega = \frac{P_o}{m_o v_{dyn}} \tag{36}$$

from which the eccentric moment is computed by

$$K = \frac{m_o v_{dyn}}{\psi \omega} \tag{37}$$

In stating the equations in this way, we have dispensed with many of the inequalities used in the original method. It was the intent of Savinov and Luskin (1960) (as evidenced by their worked examples) to 'bump up' values of K and ω to insure performance and also because it is not practical to perfectly match equipment to every application.

At this point another requirement for the system is introduced: the values of q are specified as shown in Table 3. This is the one place where this method clearly addresses the requirements of the cyclic method presented earlier. Comparison of this shows with Figure 13 shows that the range of q for steel sheet piles, which would have lower toe resistances, is most suited for the 'blue' region of Figure 13 where the toe resistance ratio γ is at its minimum and increases for other types of piles which would expect higher toe resistances. The values of q shown in the table include the effects of static weight in the suspension.

Pile Type	q_{min}	q_{max}
Steel Sheet Piles	0.15	0.5
Light Piles	0.3	0.6
Heavy and Tubular Piles	0.4	1.0

Table 3
Minimum and Maximum Values of q by the Method of Savinov and Luskin (1960)

The method has provision to compute R and by extension γ, but variations in piles and soils make parametric analysis of this difficult.

The third objective is really not met in that the method of Savinov and Luskin (1960) does not produce an estimate for the sinking velocity of the pile (but see the discussion below.) The method does deal with the power issue, which (as anyone involved intensively with vibratory pile driving understands) is critical for successful sinking of piles. This method has provision for internal losses in the system. Of greater interest is the method by which power requirements for the pile-soil system, and basically Equation 19 (with an addition for internal losses) is used to insure sufficient power for vibration.

Discussion and Special Topics

Computation of Sinking Velocity

It has been noted that the method of Savinov and Luskin (1960) does not have a way of estimating the sinking or extraction velocity of the pile driver/pile/soil system. Vibratory driving has been modelled either as a cycle-by-cycle phenomenon (as is done here) or as a continuous process; the latter is very much in evidence in A. E. Holeyman (2000); Warrington (1990). With the cyclic model, each complete rotation of the eccentrics is modelled as an independent interaction between vibrating system and the soil, assuming steady state conditions so that the final conditions of the previous cycle and the initial conditions of the current one are identical. In this respect the approach of this model is closer to the impact-by-impact approach we see in, say, the wave equation analysis used for impact hammers. However, the use of average penetration speed to monitor the performance of the system (as opposed to the blow-by-blow set approach) is more practical for field use.

The two are related, and this can be seen by considering the 'free-hanging' case. If Equation 13 is reduced to that case by setting $q = f = \gamma = \tau_o = v_o = y_o = \alpha = 0$, it becomes

$$y(\tau) = \sin(\tau) \tag{38}$$

Since $-1 \leq \sin(\tau) \leq 1$, it is apparent that $y = 1$ at the 'half-amplitude' of the system, which is given by the equation

$$A_p = \frac{K}{m_0} \tag{39}$$

The average speed of advance is thus the advance of the system per cycle times the number of cycles per unit time, or

$$v_{av} = yA_p\theta = \frac{yK\theta}{m_o} \tag{40}$$

where

$$\theta = \frac{\omega}{2\pi} \tag{41}$$

With this, it is possible to first employ the method of Savinov and Luskin (1960) to estimate the parameters and then use the cyclic method described earlier to estimate the penetration speed and compare other results. For this to be successful the assumptions of the model need to correspond with the physical reality of the system, and the value of f needs to be determined as well.

Power Requirements and Equipment Configuration

Comparing Equation 19 to the result shown in Figure 15 raises the question about what the actual maximum value of α_p really is. The issue of power requirements of vibratory pile drivers is discussed in Warrington (2006), where values of α_p for Vulcan hammers (following the lead of other American manufacturers) were higher than their Soviet counterparts. There are two things to observe about this issue.

First, in comparing Figures 9 and 15, the values of f and q were chosen in the region of the optimal region of the mode, where both γ_{min} and α_p tend to be at their lowest. Evidently those who used this model designed equipment to operate in this mode, where toe resistance is at a minimum and shaft friction was higher, which would be true for sheeting and other low displacement piling.

Second, it is possible to increase the absolute advance of the pile per rotation of the eccentrics, all other things being equal, by increasing the half amplitude of the system, as is evident in Equation 40. This is done by raising the eccentric moment K and decreasing the frequency ω, which would decrease the power consumption according to Equation 18. The Soviets developed vibrators for their heavier piles (casings, concrete cylinder piles) in just such a configuration, as described by Erofeev et al. (1985); Tseitlin et al. (1987); Warrington (1992). The downside to this is that lowering the frequency lowered the number of blows (an accurate statement for toe resistance) by the vibrating system on the soil, and thus slowed the advance of the driver.

Having said all of this, the question remains as to why the two countries/systems went in different directions as to the development of their vibratory pile driving equipment. The answer to that question may lie more in economics than in technical requirements.

The Soviets developed a wide variety of vibratory pile drivers for their construction requirements. As long as the level of work is high, it is possible for the utilisation of the equipment to remain high, although utilisation was probably not a high priority in their economic system. The equipment made good use of the power furnished to it but it did not take into consideration other factors, for example energy expended by the extended time of pile sinking.

In the U.S., utilisation becomes a much more important factor, and it is desirable for one tool to drive a wider variety of piles. One way of making this a reality is to increase the power available to the system, which would allow the machine to deal with higher soil resistances, especially the toe resistance. Such a machine is more useful to the contractor, and certainly more useful to the renter in a system where equipment rental is an important part of equipment management.

As conditions change, for example if energy becomes more expensive and/or scarcer, it is possible for the equipment to change as well. And of course there are other factors, such as the losses in the hydraulic/electric systems of mobile equipment, which are frequently overlooked in the analysis of these machines. But each design configuration was based on rational assessments of the economics and construction realities of its respective system.

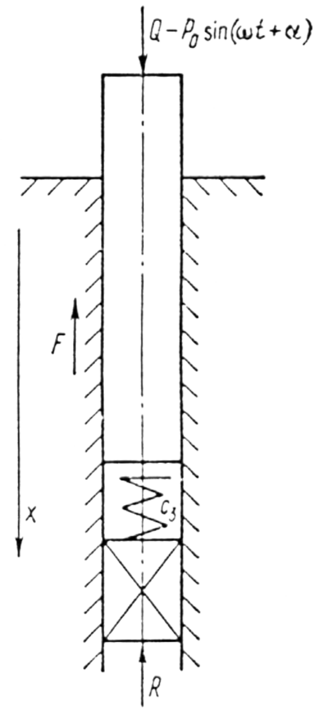

Figure 17. Vibratory model with toe elasticity (from Tseitlin et al. (1987))

Conclusions

1. The cyclic model analysed here is probably the simplest one of its kind for vibratory pile driving. It shows the various stages which take place during one cycle of the eccentrics, especially since the model was solved in a piecewise fashion. Within its limitations, it is capable of estimating the advance of the system during one eccentric cycle. It depends on other sources of information for the actual soil resistances along the shaft and the toe.

2. The greatest weakness of the model (after its lack of estimate of the shaft and toe resistances) is the use of the purely plastic soil resistance model. This is especially true for the pile toe; much of the ‘existence of the mode’ problem and the minimum toe resistance for a workable model could probably be avoided with the use of an elastic-plastic model of some kind at least at the pile toe.

3. Adding power consumption estimates to the model demonstrates that the ‘classical’ approach of Warrington (1994) has deficiencies which justify the additional power which current vibratory hammers normally possess. On the other hand, for equipment which does not normally drive piles with high toe resistances, the ‘classical’ approach still has validity, and may be useful if the economic regime in which the equipment operates changes.

4. The method of Savinov and Luskin (1960) basically avoids the issue of shaft resistance softening by requiring that the dynamic force of the vibratory pile driver be greater than the full shaft resistance. This is reasonable given the variations in the reduction between the full static resistance of the pile and the resistance seen during driving, a reduction that was not quantified at the time the method was developed and is not fully quantified now. The method’s handling of the values of q and the results of the cyclic method can be related to each other. The power estimate has the same limitations described earlier. The cyclic method–or one like it–could be used to address the Savinov and Luskin (1960) method’s greatest deficiency: the lack of a method to estimate the penetration velocity.

Postscript

Tseitlin et al. (1987) do not end their presentation on longitudinal oscillations with the method described in this paper. This postscript is a brief summary of the rest of their treatment of the subject.

The problem with the purely plastic pile toe was as evident to these authors as it is to us. They addressed this by constructing the model shown in Figure 17. Although the results were interesting, the main deficiency in the model was that there was no provision for plasticity at the pile toe, which means that the steady-state advance of the system during driving cannot be estimated.

From here the subject of using a vibrator for extracting piles (an important application of the technology) is discussed. The allows another treatment of the topic of Figure 4: the progressive loosening of the soil during the start of vibration. That led to the last topic considered, namely the sinking and extraction of long piles. With these piles the need for an elastic-purely plastic model for both shaft and toe became evident. Also evident was the need to incorporate the effects of a multi-layered soil. The two are related: each layer has different quakes and reduction factors. As long as a purely plastic model is employed, the quakes are irrelevant and the layer shaft resistances can be combined. With an elastic-plastic model, this combination is difficult to properly condense.

The solution was to develop a numerical method where the hammer-pile system is divided into discrete spring-mass elements. Those corresponding to the soil layers were divided with those layers in consideration, and solved using a method derived from a Taylor series expansion. (Most numerical methods can be derived in this way.) This is remarkable considering that the wave equation analysis–which is basically what we're talking about here–was not employed to the analysis of impact-driven piles in a broad way in the Soviet Union.

But such is beyond the scope of this paper. The development of vibratory technology for the installation of deep foundations and retaining walls is one of the great advances of construction, the result of a concerted effort that was largely shielded from the world outside the Soviet Union until it was well advanced. The story of its present advancement must and is being continued. As Dostoyevsky (1866) noted at the end of his work, set in the same place as much of this research, but with a higher purpose:

> That is the beginning of a new story, though; the story of a man's...acquaintance with a new reality of which he had previously been ignorant. That would make the subject of a new story; our present story is ended.

Nomenclature

$\aleph$	Soil resilience coefficient, 0.6-0.8 for low-frequency (5-10 Hz) pile drivers and 1 for all others
α	Phase angle, radians
α_p	Dimensionless power coefficient
$\Delta E'_{cyc}$	Dimensionless energy delivered to the soil during one cycle of the eccentrics
ΔE_{cyc}	Energy delivered to the soil during one cycle of the eccentrics, J
γ	Ratio of toe resistance to dynamic force
γ_{min}	Minimum value of γ for a system to operate in the mode
ω	Angular rotation speed, $1/sec$
ϕ	Angle of P_o at a given time, radians
ϕ_n	Starting dimensionless angle for a specific stage $n = 1, 2, 3, 4, 5$ of the cycle
ψ	Coefficient based on pile type, 0.8 for reinforced concrete piles and 1 for all others
τ	Dimensionless time
τ_n	τ_o for a specific stage $n = 1, 2, 3, 4, 5$ of the cycle
τ_o	Initial dimensionless time for a stage of the cycle
θ	Vibrating frequency of system, Hz
A_g	Peak acceleration of the ground, g's
A_o	Minimum amplitude required for successful driving, m
A_p	Half-amplitude of free-hanging system, m
A_p	Peak acceleration of the pile, g's
c	Acoustic speed of pile material, m/sec
F	Shaft resistance of soil, N
f	Ratio of shaft friction to dynamic force
F'	Soil resistance before the start of driving, N
f'	Dimensionless soil resistance before the start of driving
g	Acceleration due to gravity, m/sec^2
i_n	Direction integer for force component
L	Length of pile, m
m_o	Vibrating weight of hammer-pile system, kg
N	Power consumed by pile-soil interaction, W
n	Peak acceleration of free-hanging system during vibration, g's
P_o	Dyanmic force of rotating eccentrics, N
Q	Static force of hammer-pile system (including weight of both static and dynamic portions of the vibratory driver,) N
q	Ratio of static weight to dynamic force
Q_o	Static weight of vibrating portion of system, N

q_{min}, q_{max} Minimum and maximum permissible values of q

R Toe resistance of soil, N

s Laplace transform variable for τ

t Time, seconds

T Period between peaks of dynamic force, sec

v_n v_o for a specific stage $n = 1, 2, 3, 4, 5$ of the cycle

v_o Initial dimensionless velocity for a stage of the cycle

v_{av} Average velocity of installation or extraction of piles, m/sec

v_{dyn} Peak free-hanging velocity of system, m/sec

X Reduced displacement, m

x Displacement, m

y Maximum displacement of system, m

$y(\tau)$ Dimensionless displacement as a function of time

y_n y_o for a specific stage $n = 1, 2, 3, 4, 5$ of the cycle

y_o Initial dimensionless displacement for a stage of the cycle

References

Barkan, D. (1957, August). Foundation and drilling by the vibration method. *Proceedings of the Fourth International Conference on Soil Mechanics and Foundation Engineering*, *2*, 3–7.

Bronshtein, I., & Semendyayev, K. (1971). *A guide-book to mathematics*. Frankfurt-am-Main, Germany: Verlag Harri Deutsch.

Dostoyevsky, F. (1866). *Prestupléniye i nakazániye (crime and punishment)*. The Russian Messanger.

Erofeev, L., Smorodinov, M., Fedorov, B., Vyazovkii, V., & Villumsen, V. (1985). *Maschini i oborudanie dlya ustroiva osnovanii i fundamentov (machines and equipment for the installation of shallow and deep foundations)* (Second ed.). Moscow, Russia: Mashinostrenie.

Gumenskii, B., & Komarov, N. (1959). *Vibroburenie gruntov (soil drilling by vibration)*. Moscow, Russia: Ministry of Municipal Services of the RSFSR.

Holeyman, A., Bertin, R., & Whenham, V. (2013). Impedance of pile shafts under axial vibratory loads. *Soil Dynamics and Earthquake Engineering*, *44*, 115–126. doi: 10.1016/j.soildyn.2012.09.006

Holeyman, A. E. (2000). Keynote lecture: Vibratory driving analysis. *Application of Stress-Wave Theory to Piles*.

James, M., Smith, G., Wolford, J., & Whaley, P. (1989). *Vibration of mechanical and structural systems*. New York, NY: Harper and Row.

Kreyszig, E. (1988). *Advanced engineering mathematics* (Sixth ed.). New York, NY: John Wiley & Sons, Inc.

Levkin, M. (1960). Use of the vibratory method for sinking piles and shells in bridge construction in the ussr. *Highway Research Board Special*(60), 72–79.

Loehr, J., Lutenegger, A., Rosenblad, B., & Boeckmann, A. (2016). *Geotechnical site characterization: Geotechnical engineering circular no. 5* (No. FHWA NHI-16-072). Washington, DC: Federal Highway Administration.

Massarsch, K. R., Fellenius, B. H., & Bodare, A. (2017). Fundamentals of the vibratory driving of piles and sheet piles. *geotechnik*, *40*(2), 126–141. doi: 10.1002/gete.201600018

Rebrik, B. (1966). *Vibrotekhnika v burenii (vibro-technology for drilling)*. Moscow, Russia: Nedra.

Savinov, O., & Luskin, A. Y. (1960). *Vibratsionnyy metod pogruzheniya i yego primeneniye v stroitel'stve (vibratory method of installation and its application to construction)*. Leningrad, USSR: Gosstroyizdat.

Tseitlin, M., Verstov, V., & Azbel, G. (1987). *Vibratsionnaya tekhnika i tekhnologiya v svainykh i burovikh rabotakh (vibratory methods and the technology of piling and boring work)*. Leningrad, USSR: Stroiizdat, Leningradskoe Otdelenie.

Viking, K. (2002). *Vibro-driveability - a field study of vibratory driven sheet piles in non-cohesive soils* (Unpublished doctoral dissertation). Royal Institute of Technology.

Warrington, D. C. (1990, January). Methods for analysis of the drivability of piles by vibration. *Sixty-Ninth Annual Meeting of the Transportation Research Board*.

Warrington, D. C. (1992, October). Vibratory and impact-vibration pile driving equipment. *Pile Buck*(Second Issue), 2A–28A.

Warrington, D. C. (1994, August). Survey of methods for computing the power transmission of vibratory hammers. *Pile Buck*(Second Issue).

Warrington, D. C. (2006, September). Development of a parameter selection method for vibratory pile driver design with hammer suspension. *Colloquium of the Department of Mathematics of the University of Tennessee at Chattanooga*.

Warrington, D. C. (2019a, July). *Application of the stadyn program to analyze piles driven into sand* (Tech. Rep.). doi: 10.13140/RG.2.2.22311.09125/1

Warrington, D. C. (2019b, April). Effective hyperbolic strain-softened shear modulus for driven piles in clay. *University of Tennessee at Chattanooga, 2019 Research Dialogues*.

Warrington, D. C. (2020). *Otc 5395 revisited: Analysis of cushioned pile hammers* (Tech. Rep.). doi: 10.13140/RG.2.2.10487.04002/1